Lawrence Berkeley National Laboratory

Title
Switching between Magnetic Bloch and Néel Domain Walls with Anisotropy Modulations

Permalink
https://escholarship.org/uc/item/5cz0j3rg

Authors
Franke, Kévin JA
Ophus, Colin
Schmid, Andreas K
et al.

Publication Date
2021-04-26

Peer reviewed

Switching between Magnetic Bloch and Néel Domain Walls with Anisotropy Modulations

Kévin J. A. Franke,[1] Colin Ophus,[2] Andreas K. Schmid,[2] and Christopher H. Marrows[1]

[1]*School of Physics and Astronomy, University of Leeds, Leeds LS2 9JT, United Kingdom*
[2]*National Center for Electron Microscopy, Molecular Foundry,*
Lawrence Berkeley National Laboratory, Berkeley, California 94720, USA
(Dated: April 27, 2021)

It has been shown previously that the presence of a Dzyaloshinskii-Moriya interaction in perpendicularly magnetized thin films stabilizes Néel type domain walls. We demonstrate, using micromagnetic simulations and analytical modeling, that the presence of a uniaxial in-plane magnetic anisotropy can also lead to the formation of Néel walls in the absence of a Dzyaloshinskii-Moriya interaction. It is possible to abruptly switch between Bloch and Néel walls via a small modulation of both the in-plane, but also the perpendicular magnetic anisotropy. This opens up a route towards electric field control of the domain wall type with small applied voltages through electric field controlled anisotropies.

The presence of an interfacial Dzyaloshinskii-Moriya interaction (DMI) in perpendicular (denoted "PP") magnetized thin films stabilizes Néel type domain walls (DWs) of fixed chirality[1,2] as opposed to the Bloch DWs favored by magnetostatics that are formed in the absence of a DMI.[3] Néel DWs of fixed chirality have been shown to be driven efficiently in the same direction as the conventional electric current by spin-orbit torques,[4,5] making them appealing for potential DW devices.[6]

At the same time, electric field control of magnetism holds the promise of low-power spintronic devices. Particularly the modulation of both in-plane (IP) and PP magnetic anisotropies is well-established. Control is achieved either via interfacial strain transfer from a ferroelectric or piezoelectric substrate and inverse magnetostriction,[7–11] or via direct charge modulation at the interface with an insulator.[12–16] The latter modulates the interface anisotropy, which arises from the broken translational symmetry at the interface and spin-orbit coupling (SOC), and can give rise to PP magnetic anisotropy (PMA).[17,18]

Broken spatial inversion symmetry and SOC are also the ingredients that give rise to the DMI. It emerges at the interface of a ferromagnet with a heavy metal,[19] or more generally at the interface with a different material due to Rashba SOC, as a result of the electrostatic potential difference between the materials.[20] The latter induces a DMI at the interface between a ferromagnetic film and an insulator, and can thus be sensitive to a gate voltage.[21–26] This has been used for electric field control of magnetic DW motion via the modulation of the DMI.[27,28] The DMI has also been shown to be sensitive to the application of strain,[25,29] which opens up the route towards electric field control of DMI via coupling to a piezoelectric or ferroelectric substrate. Still, both mechanisms for tuning the DMI will also affect the magnetic anisotropy, making it difficult to disentangle their effect on magnetic DWs. Furthermore, a switch between DW types (Bloch and Néel), or a reversal of chirality with voltage remains elusive.

Recently, Chen *et al.*[30] reported that in a magnetic multilayer exhibiting PMA and DMI, the type of DW depends on the relative angle between the DW and a uniaxial IP magnetic anisotropy (IMA) of constant magnitude. Given the strong dependence of spin-orbit torques on DW type and the fact that magnetic anisotropies can be induced and modulated in various ways,[3] this observation raises the question about control – and possibly switching – of DW type with anisotropy modulations.

In this letter, we therefore demonstrate an alternative mechanism for the control of DW type: using micromagnetic simulations and analytical modeling, we show that the presence of a uniaxial IMA of fixed orientation can also lead to the formation of Néel DWs in the absence of a DMI. It is possible to abruptly switch between Bloch and Néel DWs via a small modulation of the strength of both the IMA and PMA. This opens up a route towards efficient electric field control of the DW type with small applied voltages, as the magnetic anisotropy strength can be modulated via the direct voltage controlled magnetic anisotropy mechanism,[13,14] or via magnetoelastic anisotropy induced through coupling to a piezoelectric element.[9,31]

We investigated this control of DW type through micromagnetic simulations using the OOMMF software package.[32] The simulated geometry is sketched in Fig. 1: it consists of a thin film of thickness $t = 1$ nm. Two-dimensional periodic boundary conditions[33] are used to simulate an infinite film. Simulations are initialized such that two DWs are stabilized. We choose reasonable values for the saturation magnetization $M_s = 1 \times 10^6$ A/m and exchange stiffness $A = 3 \times 10^{-11}$ J/m.[34–36] We consider the effects of a PMA with anisotropy constant K_{pp}, a uniaxial IMA along the x-direction (perpendicular to the DWs) with anisotropy constant K_{ip}, and an interfacial DMI with constant D.

To simulate a nanowire geometry, the two-dimensional periodic boundary conditions are omitted and the width of the simulations altered in the y-direction. The extent of simulations in the x-direction is chosen such that DWs
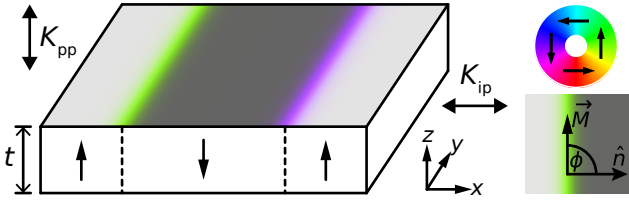
FIG. 1. (left) Sketch of the simulation geometry with definition of directions. (right) Definition of in-plane color wheel and domain wall magnetization angle ϕ between the magnetization $\vec{M}$ at the centre of the domain wall and the normal $\hat{n}$ to the domain wall.
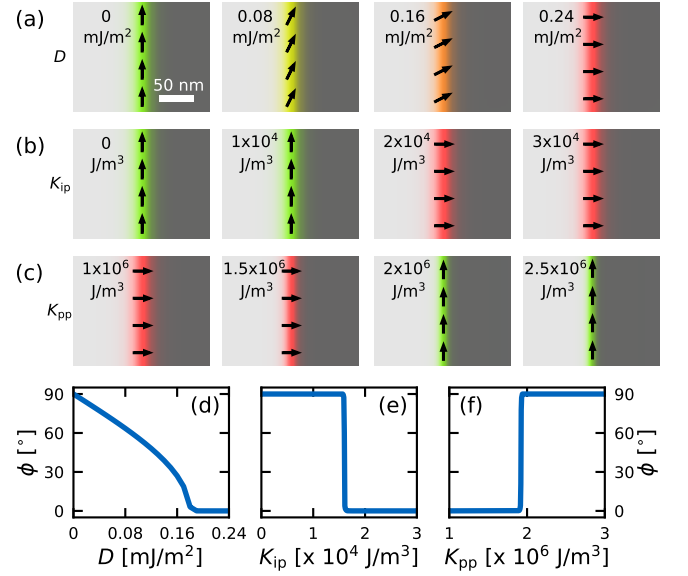

FIG. 2. Domain wall images as a function of (a) DMI constant D and (b) in-plane anisotropy constant K_{ip} for a perpendicular anisotropy constant $K_{\mathrm{pp}} = 1 \times 10^6$ J/m^3. (c) Images as a function of K_{pp} for $K_{\mathrm{ip}} = 3 \times 10^4$ J/m^3. Corresponding domain wall magnetization angles ϕ as a function of (d) D, (e) K_{ip}, and (f) K_{pp}.

are not affected by finite size effects along this dimension. The DW magnetization angle ϕ is defined relative to the DW normal $\hat{n}$ (Fig. 1). For Bloch DWs $\phi = \pm 90°$, while for Néel DWs $\phi = 0°$ or $180°$. The DW width $\delta = \int_{-\infty}^{+\infty} \cos^2(\theta) dx$ is defined as an integral over the magnetization profile of the DW, where $\theta = \sin^{-1}(M_{\mathrm{z}}/M_s)$ is the polar angle between the magnetization direction and the film normal.[37] For an ideal Bloch DW this definition yields $\delta = 2\sqrt{A/K}$.[3]

We start by reproducing the well-known effect the DMI has on the chirality of magnetic DWs in PP magnetized thin films. Images of a DW as a function of increasing DMI constant D for $K_{\mathrm{pp}} = 1 \times 10^6$ J/m^3 are shown in Fig. 2(a). The corresponding ϕ is plotted in Fig. 2(d). As reported previously,[1] the DW magnetization angle rotates continuously from a Bloch towards a Néel configuration as soon as a DMI is present. Above a certain value of D, ϕ saturates at 0, i.e. a Néel DW.

In the absence of a DMI, an IMA with easy axis perpendicular to the DW also allows for a tuning between Bloch and Néel DWs. The effect of an increasing IMA is shown in Fig. 2(b). Unlike the DMI, the anisotropy does not immediately affect the DW magnetization angle. As a function of increasing K_{ip}, the DW first remains of Bloch type until it switches abruptly to a Néel DW. This behaviour is highlighted in Fig. 2(e), where ϕ is shown as a function of K_{ip}. Note, that the magnitude of the IMA required to switch between DW types is about two orders of magnitude smaller than the PMA strength and does thus not significantly affect the magnetization in the domains.

For $K_{\mathrm{pp}} = 1 \times 10^6$ J/m^3 and $K_{\mathrm{ip}} = 3 \times 10^4$ J/m^3, a Néel DW is stabilized. As shown in the images of Fig. 2(c), and the graph in panel (f), an increase in the PMA strength eventually leads to an abrupt switch to a Bloch DW. It is thus possible to switch between DW types by either tuning the IMA or PMA strength. We further investigate this in a phase diagram (Fig. 3(a)), establishing regions where Néel or Bloch DWs are stabilized as a function of K_{pp} and K_{ip}. We find that for higher values of K_{ip} and lower values of K_{pp}, Néel DWs form. Conversely, for smaller values of K_{ip} and larger values of K_{pp}, Bloch DWs are observed. The transition between Bloch and Néel DWs appears sharp, which is in stark

contrast to the continuous transition observed when the DMI constant is changed. A $K_{\mathrm{pp}} - \mathrm{vs} - D$ phase diagram in the Supplemental Information[38] (SI) furthermore reveals that in the presence of a DMI, but absence of IMA, a tuning of the magnitude of K_{pp} has no effect on the DW magnetization angle. It is thus only this new mechanism, involving an IMA, that allows for switching between DW types via a modulation of the PMA strength.

We investigate this surprising result further by plotting the IMA strength at which the transition occurs as a function of the effective PMA (blue line in Fig. 3(b)). We find a linear dependence of $\log(K_{\mathrm{ip}})$ on $\log(K_{\mathrm{pp,eff}})$ with slope $s = 1/2$. The IMA strength at which the switch between DW types occurs thus shows a square root dependence on the effective PMA strength.

To understand this dependence, we construct a simple analytical model. The full derivation can be found in the SI.[38] The model compares the total energies of Bloch and Néel DWs for a given magnitude of K_{pp} and K_{ip}. The widths of both Néel and Bloch DWs are shown as a function of $K_{\mathrm{pp,eff}}$ in Fig. 3(c), along with the theoretical value $\delta = 2\sqrt{A/K_{\mathrm{pp,eff}}}$. We find excellent agreement between them, and therefore make the simplification that both types of DW types exhibit the same width.

We find that in first approximation the difference in DW surface energy σ between Néel (σ_{N}) and Bloch (σ_{B}) DWs is given by:

$$\Delta\sigma = \sigma_{\mathrm{N}} - \sigma_{\mathrm{B}} = K_{\mathrm{ip}} \delta - \frac{\ln 2}{\pi} \mu_0 M_{\mathrm{s}}^2 t. \qquad (1)$$
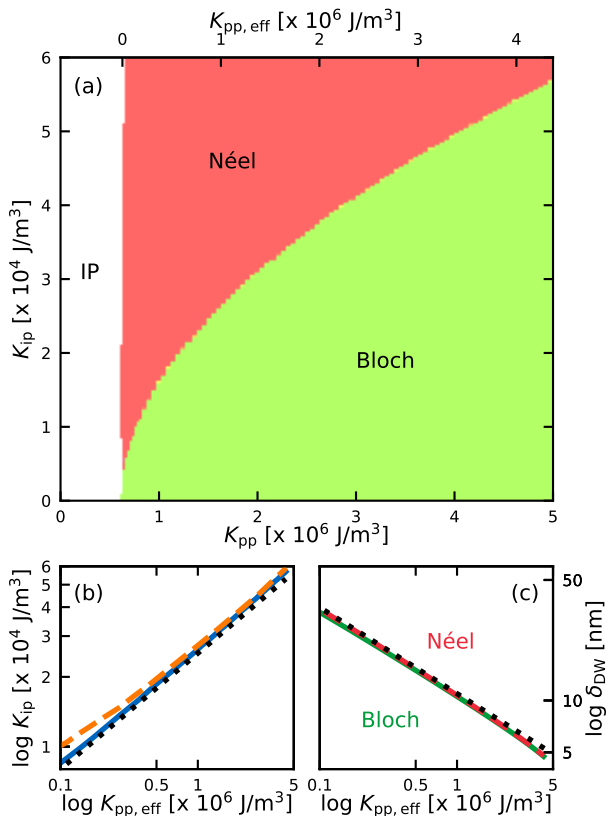
The first term results from the IMA, while the second

FIG. 3. (a) Phase diagram of the domain wall magnetization angle ϕ as a function of perpendicular (K_{pp}) and in-plane (K_{ip}) anisotropy constants. (b) Location of the transition between Bloch and Néel walls for a thin film (blue line), for a nanowire (orange dashed line), and according to the analytical model (black dotted line). (c) Widths δ of Bloch (green line) and Néel (red dashed line) domain walls just below and above the transition. The analytical expression $\delta = 2\sqrt{A/K_{pp,eff}}$ is shown as a black dotted line.

FIG. 4. (a) Phase diagram of the domain wall magnetization angle ϕ as a function of perpendicular magnetic anisotropy constant K_{PP} and nanowire width w. (b) Domain wall images as a function of K_{pp} for $w = 32$ nm.

term is a consequence of magnetostatics. The magnetostatic contribution arises from magnetic volume charges, while surface charges do not play a role. For low values of K_{ip}, the magnetostatic energy favoring Bloch DWs dominates. At large values of K_{ip}, the anisotropy energy favoring Néel DWs overcomes the magetostatic energy. The transition between DW types is expected to occur when the difference in energy is zero. As a result, the DW is expected to switch between Bloch and Néel type when:

$$K_{ip} = \frac{\ln 2\,\mu_0}{2\,\pi} \frac{M_s^2\,t}{\sqrt{A}}\sqrt{K_{pp,eff}}. \quad (2)$$

This dependence is plotted in Fig. 3(b), where excellent agreement between results from micromagnetic simulations (blue line) and the analytical model (black dotted line) is observed. The analytical model thus explains the square root dependence of the IMA strength at which the switch between DW types occurs on the effective PMA
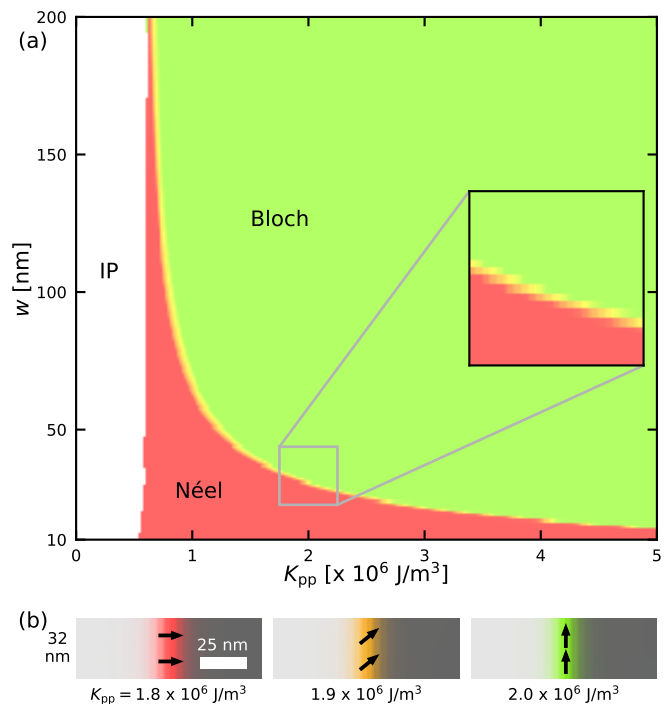
strength. The fact that the type of DW that is stabilized also depends on K_{pp} is due to the fact that the IMA contribution in $\Delta\sigma$ (Eq. 1) depends on the DW width, which in turn depends on the PMA.

Our simulations correspond to an experimental system where IP and PP magnetic anisotropies can be tuned independently. Electric field control of DW type could be achieved by tuning the strength of one of these anisotropies with a voltage. One way would be to deposit a magnetic multilayer exhibiting PMA onto a piezoelectric substrate to induce a voltage tuneable uniaxial IMA via interfacial strain transfer and inverse magnetostriction.[11,31] Another approach, that would also allow for local control, would be to tune the PMA strength via charge modulation at an interface.[12–16] This would of course require the presence of an uniaxial IMA, which could be induced in various ways. One way to achieve this would be to simply utilize the shape anisotropy in a magnetic nanowire to induce a uniaxial IMA. DWs tend to form perpendicular to the nanowire length, while the shape anisotropy induces a uniaxial anisotropy along it, which corresponds to the geometry investigated here. Nanowires are used in most DW applications, and this approach would eliminate the need for a separate mechanism to induce the uniaxial IMA. Fig. 4(a) displays the phase diagram for the DW type as a function of K_{pp} and nanowire width w. It confirms previous observations of a transition from a Bloch to a Néel DW when the nanowire width is reduced.[39,40] It does

also show that this transition depends on the strength of the PMA. Therefore, it is possible to switch between Bloch and Néel DWs for a given nanowire width when K_{pp} is modulated. We extract the location of the transition and express it in terms of effective anisotropies.[38] The resulting curve is plotted as an orange dashed line in Fig. 3(b). It matches the results for thin films and the analytical model well, except for low values of the effective IMA and PMA strengths. We ascribe this to the fact that for wide nanowires (corresponding to a low effective K_{ip}), expressing magnetostatic effects as a simple uniaxial anisotropy is too crude an approximation.

Unlike the case of thin films, the transition between DW types in nanowires does not result from a competition between a magnetic anisotropy and magnetostatics. it is purely the results of magnetostatics: magnetic volume charges favor Bloch DWs, while magnetic surface charges on the edges of the nanowire are minimized for Néel DWs. For a given width of the nanowire, increasing K_{pp} decreases the width of the DW which leads to a reduction of magnetic surface charges. As a result, Bloch DWs become energetically favorable. Conversely, decreasing K_{pp} increases the build up of magnetic surface charges, thus favoring Néel DWs.

The nanowire geometry also allows for the stabilization of intermediate DW magnetization angles ϕ. As highlighted by the inset in Fig. 4(a), the transition between Bloch and Néel DWs is not as sharp as in the thin film case. This has already been observed as a function of w.[41] As shown in Fig. 4(b), tuning between Néel and Bloch DWs with a PMA in nanowires also involves DWs with intermediate ϕ.

Stabilizing Néel DWs with an IMA does not favor one chirality, unlike the DMI. Left- and right-handed DWs are energetically degenerate. For applications, it might be necessary to obtain Néel DWs with a fixed chirality. We now show that it is still possible to tune DW type with an anisotropy in the presence of a small DMI that yields DWs of fixed chirality. Phase diagrams as a function of K_{pp} and K_{ip} for fixed values of D are shown in the SI.[38] Here, we focus on the phase diagram as a function of D and K_{ip} for a fixed value of $K_{pp} = 1 \times 10^6$ J/m^3 shown in Fig. 5. We observe that while a positive value of K_{ip} can be used to switch from a Bloch to a Néel DW when $D = 0$, a negative value of K_{ip} tunes the Néel DW obtained for large values of D towards a Bloch DW. For values of D, where an intermediate ϕ is obtained, negative and positive K_{ip} values tune the DW towards the Bloch and Néel type, respectively. A negative K_{ip} corresponds to an easy axis along the DW. We observe furthermore that while the transition between Bloch and Néel DWs is abrupt for $D = 0$, it becomes increasingly wider as D increases. This is highlighted by the contour lines (blue) for DW magnetization angles of 15°, 45°, and 75°.

The contour lines can be obtained from our analytical model by including the DMI energy in the DW surface energy. It yields the black dotted lines in Fig. 5, showing
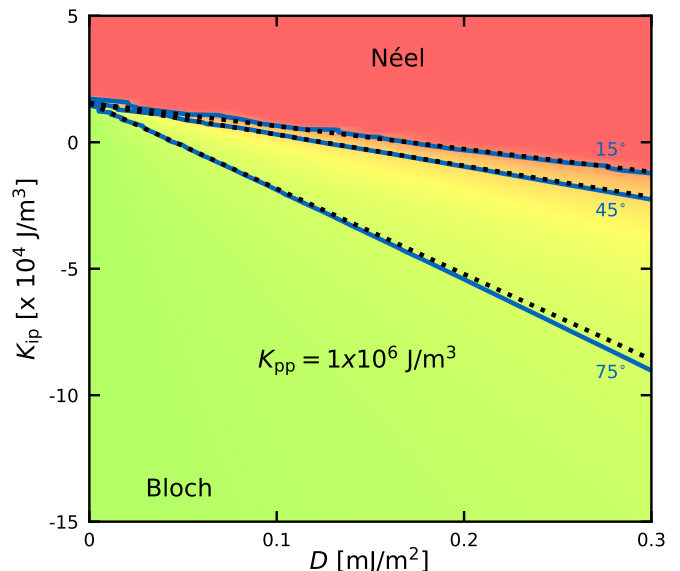

FIG. 5. Phase diagram of the domain wall magnetization angle ϕ as a function of DMI constant D and in-plane anisotropy constant K_{ip} for a fixed magnitude of the perpendicular anisotropy constant $K_{pp} = 1 \times 10^6$ J/m^3. Solid blue lines are contour lines of the simulation data for given domain wall magnetization angles of 15°, 45°, and 75°. Dotted black lines are the contour lines expected from the analytical model.

excellent agreement between micromagnetic simulations and the model, and demonstrating that the contour lines are linear in $-D$.[38]

We have therefore shown, using micromagnetic simulations, that the presence of a uniaxial in-plane magnetic anisotropy can lead to the formation of Néel domain walls in the absence of a DMI. It is possible to abruptly switch between Bloch and Néel walls via a small modulation of not only the in-plane, but also the perpendicular magnetic anisotropy. In nanowires, the shape anisotropy can be used to induce the in-plane anisotropy. In this case, tuning between domain wall types with a perpendicular magnetic anisotropy proceeds via intermediate domain wall magnetization angles. The presence of a DMI widens the transition between domain wall types. A simple analytical model accounts for the dependence of domain wall type on both the in-plane and perpendicular magnetic anisotropies, and the DMI. Our results open up the route towards voltage control of domain wall type with small applied voltages through electric field controlled anisotropies. As only Néel domain walls are driven by spin orbit torques, while Bloch domain walls are not, this could allow for efficient control of doman wall motion with electric fields.

ACKNOWLEDGMENTS

[1] A. Thiaville, S. Rohart, É. Jué, V. Cros, and A. Fert, EPL **100**, 57002 (2012).

[2] G. Chen, T. Ma, A. N'Diaye, H. Kwon, C. Won, Y. Wu, and A. Schmid, Nat. Commun. **4** (2013).

[3] A. Hubert and R. Schäfer, *Magnetic domains: the analysis of magnetic microstructures* (Springer, 1998).

[4] K.-S. Ryu, L. Thomas, S.-H. Yang, and S. Parkin, Nature Nanotech. **8**, 527 (2013).

[5] S. Emori, U. Bauer, S.-M. Ahn, E. Martinez, and G. Beach, Nat. Mater. **12**, 611 (2013).

[6] S. Parkin, M. Hayashi, and L. Thomas, Science **320**, 190 (2008).

[7] T. Lahtinen, J. Tuomi, and S. van Dijken, Adv. Mater. **23**, 3187 (2011).

[8] R. Streubel, D. Köhler, R. Schäfer, and L. Eng, Phys. Rev. B **87**, 054410 (2013).

[9] G. Yu, Z. Wang, M. Abolfath-Beygi, C. He, X. Li, K. Wong, P. Nordeen, H. Wu, G. Carman, X. Han, I. Alhomoudi, P. Amiri, and K. Wang, Appl. Phys. Lett. **106**, 072402 (2015).

[10] P. Shepley, A. Rushforth, M. Wang, G. Burnell, and T. Moore, Sci. Rep. **5**, 7921 (2015).

[11] S. Finizio, M. Foerster, M. Buzzi, B. Krüger, M. Jourdan, C. Vaz, J. Hockel, T. Miyawaki, A. Tkach, S. Valencia, F. Kronast, G. Carman, F. Nolting, and M. Kläui, Phys. Rev. Appl. **1**, 021001 (2014).

[12] M. Niranjan, C.-G. Duan, S. Jaswal, and E. Tsymbal, Appl. Phys. Lett. **96**, 222504 (2010).

[13] T. Maruyama, Y. Shiota, T. Nozaki, K. Ohta, N. Toda, M. Mizuguchi, A. Tulapurkar, T. Shinjo, M. Shiraishi, S. Mizukami, Y. Ando, and Y. Suzuki, Nature Nanotech. **4**, 158 (2009).

[14] Y. Shiota, S. Murakami, F. Bonell, T. Nozaki, T. Shinjo, and Y. Suzuki, Appl. Phys. Express **4**, 043005 (2011).

[15] W.-G. Wang, M. Li, S. Hageman, and C. L. Chien, Nat. Mater. **11**, 64 (2012).

[16] U. Bauer, L. Yao, A. Tan, P. Agrawal, S. Emori, H. Tuller, S. van Dijken, and G. Beach, Nat. Mater. **14**, 174 (2015).

[17] M. Johnson, P. Bloemen, F. den Broeder, and J. de Vries, Rep. Prog. Phys. **59**, 1409 (1996).

[18] A. Aharoni, *Introduction to the Theory of Ferromagnetism*, 2nd ed. (Clarendon Press, 2001).

[19] A. Fert and P. M. Levy, Phys. Rev. Lett. **44**, 1538 (1980).

[20] A. Kundu and S. Zhang, Phys. Rev. B **92**, 094434 (2015).

[21] K. Nawaoka, S. Miwa, Y. Shiota, N. Mizuochi, and Y. Suzuki, Appl. Phys. Express **8**, 063004 (2015).

[22] T. Srivastava, M. Schott, R. Juge, V. Křižáková, M. Belmeguenai, Y. Roussigné, A. Bernand-Mantel, L. Ranno, S. Pizzini, S.-M. Chérif, A. Stashkevich, S. Auffret, O. Boulle, G. Gaudin, M. Chshiev, C. Baraduc, and H. Béa, Nano Lett. **18**, 4871 (2018).

[23] W. Zhang, H. Zhong, R. Zang, Y. Zhang, S. Yu, G. Han, G. L. Liu, S. S. Yan, S. Kang, and L. M. Mei, Appl. Phys. Lett. **113**, 122406 (2018).

[24] J. Suwardy, M. Goto, Y. Suzuki, and S. Miwa, Jpn. J. Appl. Phys. **58**, 060917 (2019).

[25] Q. Yang, Y. Cheng, Y. Li, Z. Zhou, J. Liang, X. Zhao, Z. Hu, R. Peng, H. Yang, and M. Liu, Adv. Electron. Mater. **6**, 2000246 (2020).

[26] M. Schott, L. Ranno, H. Béa, C. Baraduc, S. Auffret, and A. Bernand-Mantel, J. Magn. Magn. Mater **520**, 167122 (2021).

[27] T. Koyama, Y. Nakatani, J. Ieda, and D. Chiba, Sci. Adv. **4** (2018).

[28] T. Koyama, J. Ieda, and D. Chiba, Appl. Phys. Lett. **116**, 092405 (2020).

[29] N. S. Gusev, A. V. Sadovnikov, S. A. Nikitov, M. V. Sapozhnikov, and O. G. Udalov, Phys. Rev. Lett. **124**, 157202 (2020).

[30] G. Chen, A. N'Diaye, S. Kang, H. Kwon, C. Won, Y. Wu, Z. Qiu, and A. Schmid, Nat. Commun. **6** (2015).

[31] S. Li, Q. Xue, H. Du, J. Xu, Q. Li, Z. Shi, X. Gao, M. Liu, T. Nan, Z. Hu, N. X. Sun, and W. Shao, J. Appl. Phys. **117**, 17D702 (2015).

[32] M. Donahue and D. Porter, *OOMMF user's guide, Version 1.0*, Interagency Report NISTIR 6376 (National Institute of Standards and Technology, Gaithersburg, MD, 1999).

[33] W. Wang, C. Mu, B. Zhang, Q. Liu, J. Wang, and D. Xue, Comput. Mater. Sci. **49**, 84 (2010).

[34] J. Stöhr and H. Siegmann, *Magnetism: From Fundamentals to Nanoscale Dynamics* (Springer, 2006).

[35] C. Eyrich, W. Huttema, M. Arora, E. Montoya, F. Rashidi, C. Burrowes, B. Kardasz, E. Girt, B. Heinrich, O. N. Mryasov, M. From, and O. Karis, J. Appl. Phys. **111**, 07C919 (2012).

[36] T. Devolder, J.-V. Kim, L. Nistor, R. Sousa, B. Rodmacq, and B. Diény, J. Appl. Phys. **120**, 183902 (2016).

[37] J. Jakubovics, Philos. Mag. B **38**, 401 (1978).

[38] Supplemental material contains additional phase diagrams and details of the analytical model.

[39] E. Martinez, L. Torres, and L. Lopez-Diaz, Phys. Rev. B **83**, 174444 (2011).

[40] M. D. DeJong and K. L. Livesey, Phys. Rev. B **92**, 214420 (2015).

[41] B. Boehm, A. Bisig, A. Bischof, G. Stefanou, B. J. Hickey, and R. Allenspach, Phys. Rev. B **95**, 180406 (2017).